

NANO EXPRESS

Open Access



Rh-doped MoTe₂ Monolayer as a Promising Candidate for Sensing and Scavenging SF₆ Decomposed Species: a DFT Study

Hongliang Zhu¹, Hao Cui^{2,3*} , Dan He⁴, Ziwen Cui⁵ and Xiang Wang^{1*}

Abstract

In this work, the adsorption and sensing behaviors of Rh-doped MoTe₂ (Rh-MoTe₂) monolayer upon SO₂, SOF₂, and SO₂F₂ are investigated using first-principles theory, wherein the Rh doping behavior on the pure MoTe₂ surface is included as well. Results indicate that T_{Mo} is the preferred Rh doping site with E_b of -2.69 eV, and on the Rh-MoTe₂ surface, SO₂ and SO₂F₂ are identified as chemisorption with E_{ad} of -2.12 and -1.65 eV, respectively, while SOF₂ is physically adsorbed with E_{ad} of -0.46 eV. The DOS analysis verifies the adsorption performance and illustrates the electronic behavior of Rh doping on gas adsorption. Band structure and frontier molecular orbital analysis provide the basic sensing mechanism of Rh-MoTe₂ monolayer as a resistance-type sensor. The recovery behavior supports the potential of Rh-doped surface as a reusable SO₂ sensor and suggests its exploration as a gas scavenger for removal of SO₂F₂ in SF₆ insulation devices. The dielectric function manifests that Rh-MoTe₂ monolayer is a promising optical sensor for selective detection of three gases. This work is beneficial to explore Rh-MoTe₂ monolayer as a sensing material or a gas adsorbent to guarantee the safe operation of SF₆ insulation devices in an easy and high-efficiency manner.

Keywords: Rh-MoTe₂ monolayer, First-principles theory, SF₆ decomposed species, Gas sensor

Introduction

SF₆ insulation devices, in high even ultra-high voltage power systems, are one kind of the most important and expensive equipment [1–3], except electrical transformers [4, 5], to guarantee the safe operation of the whole system. These contributions attribute to the strong arc-extinguishing property and high electronegativity of SF₆ gas that behaves as an insulation media in such devices [6]. However, in a long-running one, SF₆ could still be decomposed into several low-fluorine sulfides by the power of partial discharge caused by inevitable inner defects of the equipment [7, 8]. Moreover,

these by-products will further interact with the surrounding trace water and oxygen, forming some stable chemicals such as SO₂, SOF₂, and SO₂F₂ and instead deteriorating the insulation behavior of SF₆ [9]. Therefore, detecting these decomposed species has been regarded as an effective manner to evaluate the decomposing status of SF₆ and to reflect the operation status of related insulation devices [10].

With the growing attention of transition metal dichalcogenides (TMDs), MoS₂-based sensors have been proposed for detection of SF₆ decomposed species [11–13]. These reports have demonstrated the appropriateness and superiority of transition metal (TM)-doped MoS₂ monolayer for sensing components including SO₂ and SOF₂. Besides, a theoretical study on the sensing characteristic of pristine MoTe₂ monolayer upon SF₆ decomposed species proves its suitability for sensing SO₂ [14]. Moreover, recent advancements in chemical vapor

* Correspondence: cuihaocqu@163.com; xwangchn@vip.sina.com

²College of Artificial Intelligence, Southwest University, Chongqing 400715, China

¹Key Laboratory of Biorheological Science and Technology, Ministry of Education, College of Bioengineering, Chongqing University, Chongqing 400044, China

Full list of author information is available at the end of the article

deposition (CVD) used for large-scale synthesis of TMDs largely accelerate the development of MoTe₂ monolayer for gas sensing applications [15–17]. As reported, MoTe₂ monolayer possesses outstanding carrier mobility, large bond length, and low binding energy, which provides it with high sensitivity upon gas interactions at room temperature [18]. Thus, it is hopeful that MoTe₂ monolayer is quite a promising candidate for gas sensing, and its application for detection of SF₆ decomposed species should be further explored.

It is well proved that TM-doped 2D nanomaterials possess stronger adsorption performance and sensing behavior upon gaseous molecules compared with pristine surfaces [19–22]. This is because of the admirable chemical activity and catalytic behavior of TM whose *d* orbital can strongly hybridize with those adsorbed molecules, facilitating the chemisorption and enlarging the charge transfer [23–25]. When it comes to the MoTe₂ monolayer, to the best of our knowledge there have few theoretical reports on the TM-doping behavior on its monolayer; meanwhile, related adsorption and sensing behaviors of TM-doped MoTe₂ monolayer upon gases are also less explored. Among the TM elements, rhodium (Rh) with strong catalytic performance has been demonstrated as a desirable TM dopant on other nano-surfaces for gas adsorption [26, 27]. Especially, ref. [26] investigates the Rh doping behavior on the MoSe₂ monolayer and its enhanced performance for toxic gas adsorption. From this regard, it would be interesting using the first-principles theory to study the Rh doping behavior on the less explored MoTe₂ monolayer to compare their geometric property and give a better understanding of Rh doping on the TMDs. Beyond that, the adsorption and sensing performances of Rh-doped MoTe₂ (Rh-MoTe₂) monolayer upon three SF₆ decomposed species, namely, SO₂, SOF₂, and SO₂F₂, were theoretically simulated as well to explore its potential sensing application in some typical areas. The electronic and optical behaviors of Rh-MoTe₂ monolayer upon gas adsorption provide the basic sensing mechanisms for its exploration as a resistance-type or optical gas sensor to realize the detection of SF₆ decomposed species. The desorption behavior verifies the potential of Rh-MoTe₂ monolayer as a gas scavenger to remove these noxious gases in SF₆ insulation devices, which from another aspect guarantees the safe operation of the power system. This work would be meaningful to propose novel nano-sensing material and its application for evaluating the operation status of SF₆ insulation devices in an easy and high-efficiency manner.

Computational Details

All the results were obtained in the Dmol³ package [28] based on the first-principles theory. The DFT-D method

proposed by Grimme was adopted [29] to better understand the van der Waals force and long-range interactions. Perdew-Burke-Ernzerhof (PBE) function with generalized gradient approximation (GGA) was employed to treat the electron exchange and correlation terms [30]. Double numerical plus polarization (DNP) was employed as the atomic orbital basis set [31]. The Monkhorst-Pack *k*-point mesh of 7 × 7 × 1 was defined for supercell geometry optimizations, while a more accurate *k*-point of 10 × 10 × 1 was selected for electronic structure calculations [32]. The energy tolerance accuracy, maximum force, and displacement were selected as 10⁻⁵ Ha, 2 × 10⁻³ Ha/Å, and 5 × 10⁻³ Å [33], respectively. For static electronic structure calculations, self-consistent loop energy of 10⁻⁶ Ha, the global orbital cut-off radius of 5.0 Å to ensure the accurate results of total energy [34].

A MoTe₂ monolayer with supercell of 4 × 4 and vacuum region of 15 Å containing 16 Mo and 32 Te atoms was established to perform the whole calculation below. It has been proved that a 4 × 4 supercell is large enough to conduct the gas adsorption process while a 15 Å slab is proper to prevent the interaction between adjacent units [35]. Apart from that, the Hirshfeld method [36] was employed throughout this work to analyze the atomic charge of Rh dopant (*Q*_{Rh}) and molecular charge of adsorbed molecules (*Q*_T). Therefore, a positive value of *Q*_{Rh} (*Q*_T) represents that the Rh dopant (gas molecule) is an electron donor, while a negative *Q*_{Rh} or *Q*_T indicates the related electron-accepting behavior. Only the most favorable configurations of Rh-MoTe₂ monolayer and adsorption systems are plotted and analyzed in the following parts.

Results and Discussion

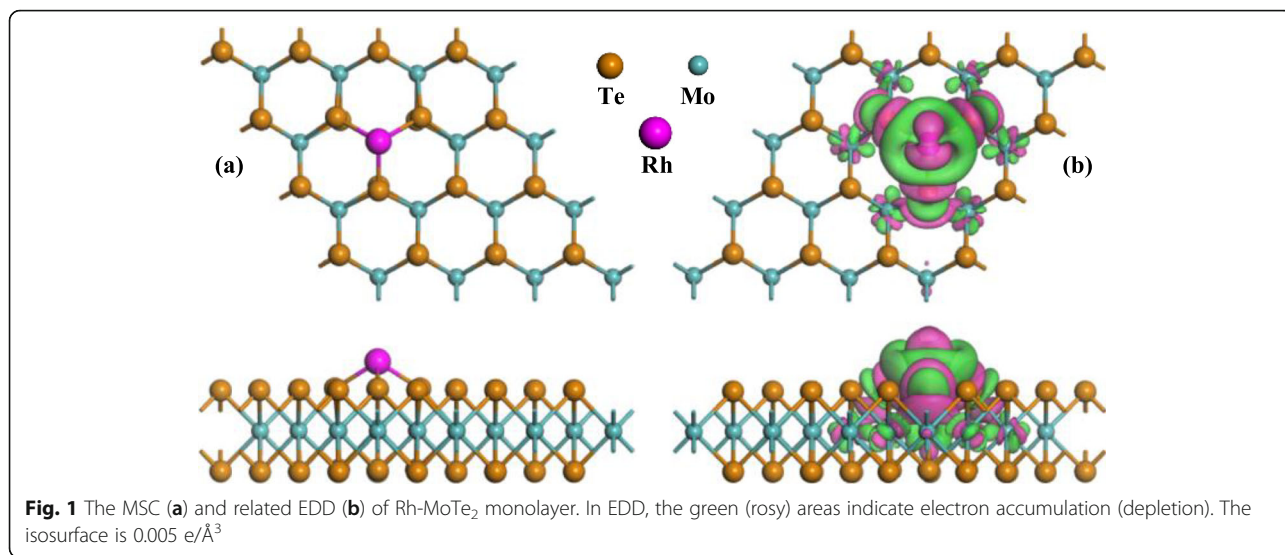
Analysis of Rh-MoTe₂ Monolayer

Upon Rh-MoTe₂ monolayer, four possible adsorption sites are considered, traced as T_H (above the center of the hexagonal ring of MoTe₂), T_{Mo} (at the top of the Mo atom), T_{Te} (at the top of Te atom), and T_B (the bridge site between two Te atoms), respectively. The binding energy (*E*_b) for Rh doping onto the MoTe₂ monolayer is formulated as:

$$E_b = E_{\text{Rh-MoTe}_2} - E_{\text{Rh}} - E_{\text{MoTe}_2} \quad (1)$$

where *E*_{Rh-MoTe₂}, *E*_{Rh}, and *E*_{MoTe₂} represent the energies of the Rh-MoTe₂ monolayer, Rh atoms, and pristine MoTe₂ monolayer, respectively.

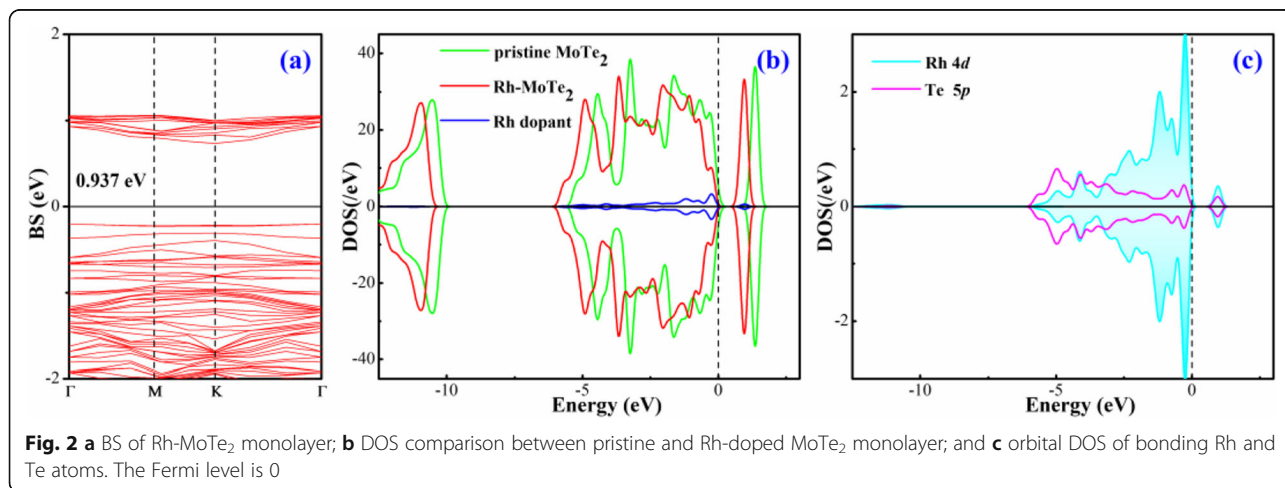
Based on this definition, the most stable configuration (MSC) with the lowest *E*_b in line with related electron deformation density (EDD) of Rh-MoTe₂ monolayer is depicted in Fig. 1. One can see that the Rh dopant is trapped on the T_{Mo} site, forming three covalent bonds



with neighboring Te atoms on the upper layer of MoTe₂ monolayer. Three Rh-Te bonds are measured equally as 2.54 Å, shorter than the sum of covalent radii of Rh and Te atoms (2.61 Å [37]), indicating the formation of chemical bonds for Rh doping on the MoTe₂ layer. The calculated E_b of this configuration is -2.69 eV, much larger than those of -2.14 eV for T_H site, -1.28 eV for T_{Te} site, and -2.55 eV for T_B site. It is worth noting that the Rh-Te bonds in Rh-MoTe₂ monolayer are longer than those of Rh-Se bonds in Rh-MoSe₂ monolayer and the E_b for Rh doping is smaller on the MoTe₂ surface in comparison with that of MoSe₂ counterpart. These indicate the stronger binding force of Rh-Se than Rh-Te bonds. Based on the Hirshfeld method, the Rh dopant behaves as an electron acceptor during doping process, which receives 0.045 e from the MoTe₂ surface proving its electron-accepting behavior in surface doping [26].

This is in accordance with the EDD in which the Rh atom is mainly surrounded by electron accumulation.

The band structure (BS) and density of state (DOS) of Rh-MoTe₂ system are depicted in Fig. 2 to better understand the caused change in electronic behavior of MoTe₂ surface by Rh doping. It is reported that pristine MoTe₂ monolayer has a direct bandgap of 1.10 eV [38]. In Fig. 2a, the bandgap of Rh-MoTe₂ monolayer is obtained as 0.937 eV according to the calculations. This indicates that the Rh dopant induces several impurity states within the bandgap of MoTe₂ system, narrowing the bandgap of the whole system accordingly. Besides, the top of the valence band is localized on the Γ point and the bottom of the conduction band is on the K point, implying the indirect semiconducting property for Rh-MoTe₂ system. In Fig. 2b, it is seen that the states of Rh dopant contribute largely to the top of the conduction



band of pristine MoTe₂ monolayer and forming several novel DOS peaks around the Fermi level. These peaks seemingly change the electronic behavior of the whole system, reducing its electrical conductivity accordingly. Because the Rh dopant is trapped on the T_{Mo} site forming bonds with Te atoms, the atomic DOS of Rh and Te atoms are plotted to understand the electron hybridization behavior between them. As shown in Fig. 2c, the Rh 4*d* orbital is strongly hybrid with the Te 5*p* orbital from -5 to 2 eV, accounting for the significant bonding interaction that leads to the formation of chemical bonds of Rh-Te.

Gas Adsorption Configurations of Rh-MoTe₂ Monolayer

Based on the relaxed structure of Rh-MoTe₂ monolayer, the adsorption of SO₂, SOF₂, and SO₂F₂ molecules onto its surface around the Rh center are fully simulated. Before that, the geometric structures of the three gas molecules should also be optimized as well, as exhibited in Additional file 1: Figure S1. The adsorption energy (E_{ad}) is used to determine the most stable configuration of each system, formulated as:

$$E_{\text{ad}} = E_{\text{Rh-MoTe}_2/\text{gas}} - E_{\text{Rh-MoTe}_2} - E_{\text{gas}} \quad (2)$$

in which the $E_{\text{Rh-MoTe}_2/\text{gas}}$ and $E_{\text{Rh-MoTe}_2}$ are the total energy of Rh-MoTe₂ monolayer before and after adsorption, whereas E_{gas} is the energy of isolated gas molecule. According to this definition, the MSC with the lowest E_{ad} could be identified.

To better understand the charge-transfer behavior during gas adsorption, EDD is also calculated for each configuration. Detailed information for SO₂, SOF₂, and SO₂F₂ adsorption could be seen in Figs. 3, 4, and 5,

respectively. In addition, the adsorption parameters including E_{ad} , charge-transfer (Q_{T}), and bond length (D) are listed in Table 1.

For SO₂ adsorption on the Rh-MoTe₂ monolayer, one can find from Fig. 3 that the SO₂ molecule is basically parallel to the MoTe₂ layer with one O atom and one S atom trapped by the Rh dopant. As listed in Table 1, the newly formed Rh-O and Rh-S bonds are measured as 2.16 and 2.36 Å, respectively, indicating the strong binding force between Rh dopant and SO₂ molecule. Besides, the E_{ad} is obtained as -1.65 eV implying the chemisorption for the SO₂ system, and the Q_{T} is obtained as -0.333 e implying the electron-withdrawing behavior of SO₂. After adsorption, the Rh dopant is negatively charged by 0.017 e, which means it contributes 0.028 e to the adsorbed SO₂ and the other part of charge (0.305) comes from the MoTe₂ monolayer. Compared with the adsorption parameters in the MoTe₂/SO₂ system ($E_{\text{ad}} = -0.245$ eV; $Q_{\text{T}} = -0.086$ e; $D = 3.44$ Å [14]), one can infer that Rh doping largely enhances the reacting behavior and electronic redistribution for the MoTe₂ monolayer upon SO₂ adsorption, making the adsorbent much desirable for gas interaction. Moreover, the S-O bonds in the SO₂ molecule are separately elongated to 1.50 and 1.58 Å after adsorption, from that uniform 1.48 Å in the gas phase; the three Rh-Te bonds in the Rh-MoTe₂ monolayer are elongated to 2.58, 2.58, and 2.64 Å, respectively. These deformations imply the geometric activation during adsorption for both nano-adsorbent and gaseous adsorbate, which further confirms the strong chemisorption here. From the EDD distribution, it is found that the SO₂ molecule is surrounded by electron accumulation, which agrees with the Hirshfeld analysis; and electron accumulation largely surrounds the

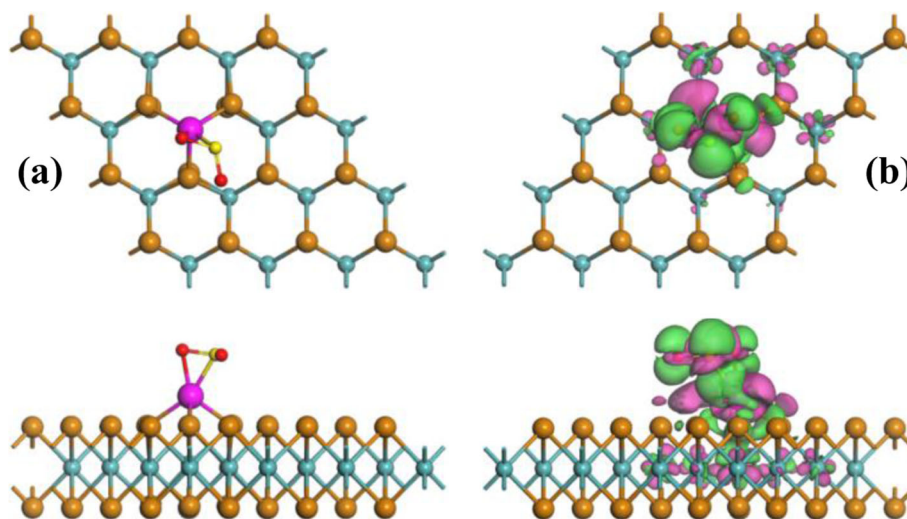


Fig. 3 MSC (a) and EDD (b) of Rh-MoTe₂/SO₂ system. In EDD, the green (rosy) areas indicate electron accumulation (depletion), with isosurface as 0.005 e/Å³

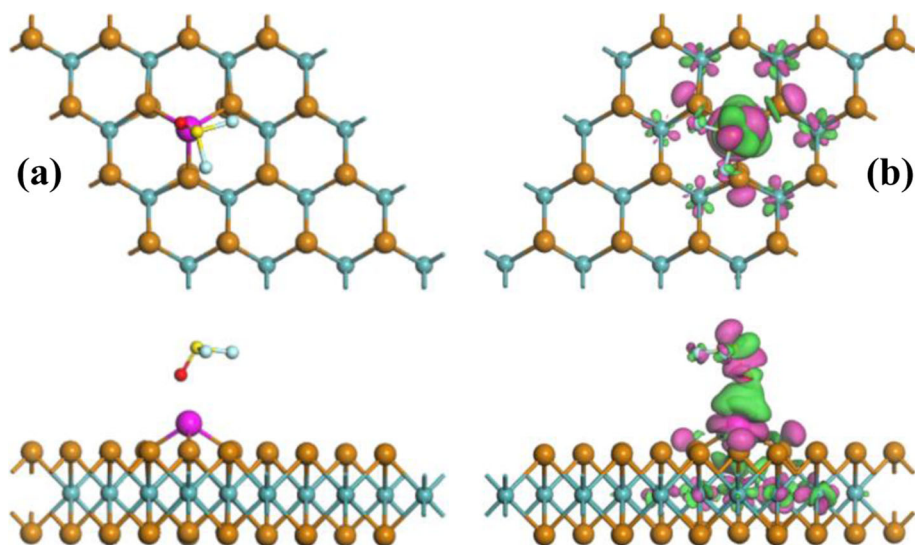


Fig. 4 Same as Fig. 3 but for Rh-MoTe₂/SOF₂ system

Rh-S and Rh-O bonds, suggesting the electron hybridization in the formation of new chemical bonds.

In the Rh-MoTe₂/SOF₂ system presented in Fig. 4, the SOF₂ molecule preferred to approach the Rh dopant by the O-end position and the plane made of the S atom and two F atoms are almost parallel to the MoTe₂ layer. However, there has no obvious evidence suggesting the formation of new bonds between Rh dopant and SOF₂ molecule. The nearest distance of Rh-O is measured to be 2.25 Å, a little longer than that in the SO₂ system, and the SOF₂ molecule does not undergo large geometric deformation after interaction. These findings manifest the relatively weaker adsorption performance of Rh-MoTe₂ monolayer upon SOF₂ in comparison with SO₂.

As presented in Table 1, the E_{ad} is calculated as -0.46 eV supporting the physisorption again [39] and the Q_T is obtained as 0.040 e implying the electron-donating behavior of SOF₂. According to the EDD, one can see that the electron accumulation is mainly localized on the area between the SOF₂ molecule and Rh dopant, which implies somewhat hybridization between them, while the electron depletion on the SOF₂ molecule agrees with the Hirshfeld analysis.

In terms of the SO₂F₂ adsorption system, as depicted in Fig. 5, it is found that after optimization, the SO₂F₂ molecule tends to be resolved to be a F atom and a SO₂F group. Both are captured by the Rh dopant forming a Rh-F bond and a Rh-S bond, respectively, with

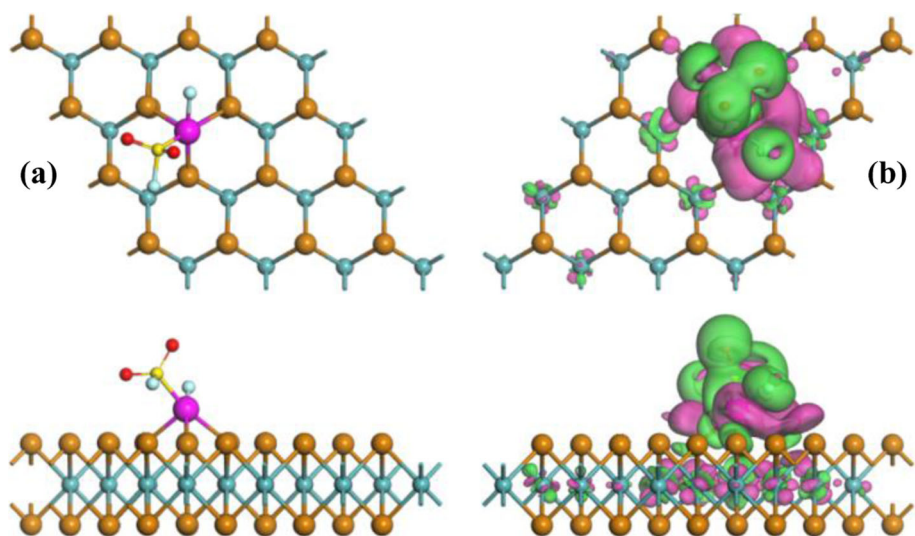


Fig. 5 Same as Fig. 3 but for Rh-MoTe₂/SO₂F₂ system

Table 1 Adsorption parameters of Rh-MoTe₂ monolayer upon SO₂, SOF₂, and SO₂F₂

Systems	E_{ad} (eV)	Q_{T} (e)	D (Å)
SO ₂ system	-1.65	-0.333	Rh-O (2.16); Rh-S (2.36)
SOF ₂ system	-0.46	0.040	Rh-O (2.25)
SO ₂ F ₂ system	-2.12	-0.753	Rh-F (2.02); Rh-S (2.26)

related bond length of 2.02 and 2.26 Å. The newly formed bonds indicate the strong binding force between Rh dopant and SO₂F₂ molecule, which combined with the calculated E_{ad} of 2.12 eV evidence the chemisorption nature for Rh-doped surface upon SO₂F₂ adsorption, similar as that in the SO₂ system. From the EDD, the electron accumulation is significantly localized on the SO₂F₂ molecule, in agreement with the result of Q_{T} (-0.753 e) based on Hirshfeld analysis. On the other hand, a large number of electron depletion is localized on the Rh dopant and a little is on the MoTe₂ monolayer. In other words, the Rh dopant contributes largely to the charge-transfer to the adsorbed SO₂F₂ molecule, manifesting its high electron mobility and strong chemical reactivity [40]. At the same time, the overlap of electron accumulation and electron depletion on the Rh-S and Rh-F bonds suggest the electron hybridization in their formation.

Based on the analysis of adsorption configuration and parameters, one can conclude that the Rh-MoTe₂ monolayer possesses the best performance upon SO₂F₂ molecule, followed by SO₂ and the last one comes to SOF₂. In the meanwhile, the Rh dopant can largely affect the electron distribution of this system and therefore dramatically alter the electronic behavior of the Rh-MoTe₂ monolayer.

Electronic Behaviors of Rh-MoTe₂ Monolayer upon Gas Adsorption

The band structure (BS) and density of state (DOS) of three adsorption systems are exhibited in Fig. 6 to comprehend the electronic behavior of Rh-MoTe₂ monolayer in gas adsorption. As above analyzed, Rh-MoTe₂ monolayer has the best performance upon SO₂F₂ adsorption. Thus, from Fig. 6 (c2), it is seen that the molecular DOS of SO₂F₂ experiences pronounced deformations, which is integrally left-shifted and some of the states combine to a large one below the Fermi level. From Fig. 6 (c3) where the orbital DOS is shown, it is seen that the Rh 4*d* orbital is highly hybrid with the F 2*p* orbital, and is somewhat hybrid with S 3*p* orbital. From this aspect, it is presumed that Rh-F bond is stronger than that of Rh-S. In the SO₂ system, the Rh 4*d* orbital is highly hybrid with the O 2*p* orbital and followed by the S 3*p* orbital in Fig. 6 (a3), and one could also presume that Rh dopant has stronger binding force with the O atom rather than

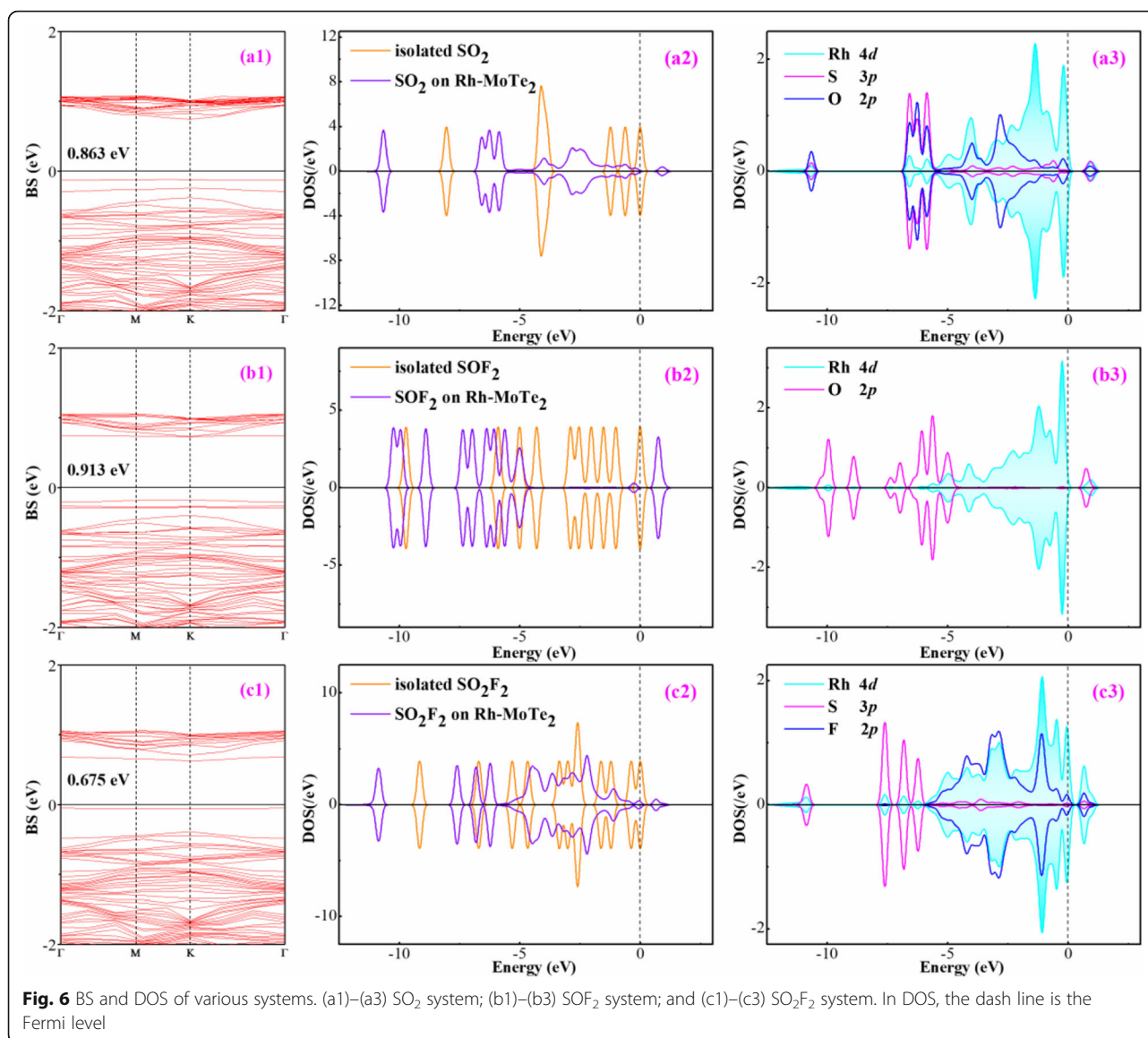
the S atom. Due to such hybridization, the molecular DOS of SO₂ in Fig. 6 (a2) suffers remarkable deformation. As for the SOF₂ system, one can see in Fig. 6 (b3) that the Rh dopant has little orbital hybridization with the nearest O atom, which supports the weak interaction for SOF₂ adsorption.

Along with the change of orbital and molecular DOS, the whole state of the gas adsorbed system would be automatically changed compared with the pure Rh-MoTe₂ system. From Fig. 6 (a1)–(c1) where the BS of the adsorbed system are portrayed, one can see that the BS in the SOF₂ system does not experience significant deformation in comparison with that of isolated Rh-MoTe₂ system, while those in the SO₂ and SO₂F₂ system are different, in which some novel states are emerged around the Fermi level, thus narrowing the bandgap largely. Detailedly, the bandgap of the Rh-MoTe₂ is reduced to 0.863, 0.913, and 0.675 eV after adsorption of SO₂, SOF₂, and SO₂F₂, respectively. This provides the basic sensing mechanism for Rh-MoTe₂ monolayer as a possible resistance-type gas sensor.

Frontier Molecular Orbital Analysis

To confirm the results based on the BS analysis, the frontier molecular orbital theory is performed to analyze the distribution and energies of frontier molecular orbitals (FMO) of isolated and gas adsorbed Rh-MoTe₂ surface. The FMO contains highest occupied molecular (HOMO) and lowest unoccupied molecular orbital (LUMO), and the energy gap between them can evaluate the electrical conductivity of the analyzed system [41]. To obtain the accurate results of the energies of FMO, the smearing in this part of calculations is set to 10⁻⁴ Å. The distributions and energies of FMO of Ru-MoTe₂ monolayer before and after gas adsorptions are described in Fig. 7.

From Fig. 7a, one can observe that the HOMO and LUMO are mainly localized at the Rh dopant, suggesting its high reactivity in the surroundings. The energies of HOMO and LUMO are obtained as -4.885 and -3.927 eV, respectively, with the calculated bandgap of 0.958 eV. After adsorption of three gas species, as seen in Fig. 7b–d, the FMO distributions of Rh-MoTe₂ surface are afflicted with different degrees of deformations, where the reaction occurs resulting in the convergence of the electron cloud. Along with these deformations, the energies of FMO have changed accordingly. It is found that the energies of FMO are decreased to different degrees after adsorption of three gases, in which those in SOF₂ system experience the largest decreases. However, the energy gap in SOF₂ system undergoes the smallest change in comparison with that of pure Rh-MoTe₂ system. Specifically, the energy gap of Rh-MoTe₂ monolayer (0.958 eV) is decreased by 0.044 eV after SOF₂



adsorption, while is reduced by 0.061 and 0.281 eV after SO₂ and SO₂F₂ adsorption, respectively. These findings indicate that the electrical conductivity of Rh-MoTe₂ monolayer will decrease after adsorption of three gases and the decrease is the most significant in the SO₂F₂ system, which agree with the conclusions from BS analysis. Besides, the energy gaps from frontier molecular orbital theory is basically close to those of bandgaps from BS results, implying the good accuracy of our calculations.

Sensing Response and Recovery Property

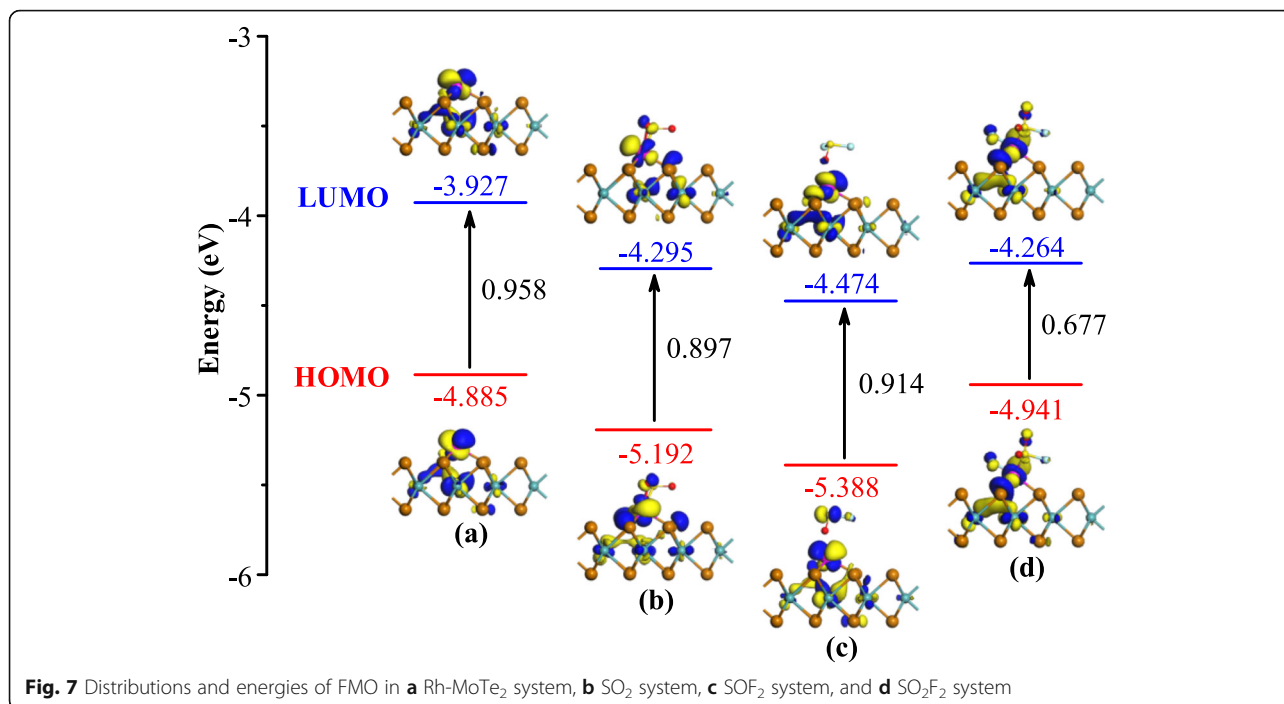
The changes in the bandgap of Rh-MoTe₂ monolayer after gas adsorption manifest its change in electrical conductivity in related gas atmosphere [42], which can provide the basic sensing mechanism for exploration of Rh-MoTe₂

monolayer as a resistance-type gas sensor. Besides, the larger change in electrical conductivity would account for a higher sensitivity for gas detection. To identify the possibility of Ru-MoTe₂ monolayer as a sensor, its conductivity (σ) and sensitivity (S) upon three typical gases are calculated using the following formulas [43, 44]:

$$\sigma = A \cdot e^{(-B_g/2kT)} \quad (3)$$

$$S = \frac{\frac{1}{\sigma_{\text{gas}}} - \frac{1}{\sigma_{\text{pure}}}}{\frac{1}{\sigma_{\text{pure}}}} = \frac{\sigma_{\text{pure}} - \sigma_{\text{gas}}}{\sigma_{\text{gas}}} \quad (4)$$

In formula 3, A is a constant, B_g is the bandgap of the analyzed system, k is the Boltzmann constant, and T is



the working temperature. In formula 4, σ_{gas} and σ_{pure} respectively mean the conductivity of analyzed adsorption system and isolated Rh-MoTe₂ monolayer. According to such two formulas, it is found that the S of certain surface could be obtained just with its bandgap before and

after gas adsorption. After calculation, the sensitivities of Rh-MoTe₂ monolayer upon SO₂, SOF₂, and SO₂F₂ detection at 298 K are 76.3, 37.3, and 99.4%, respectively. These findings suggest that the Rh-MoTe₂ monolayer possess the most admirable sensing behavior upon

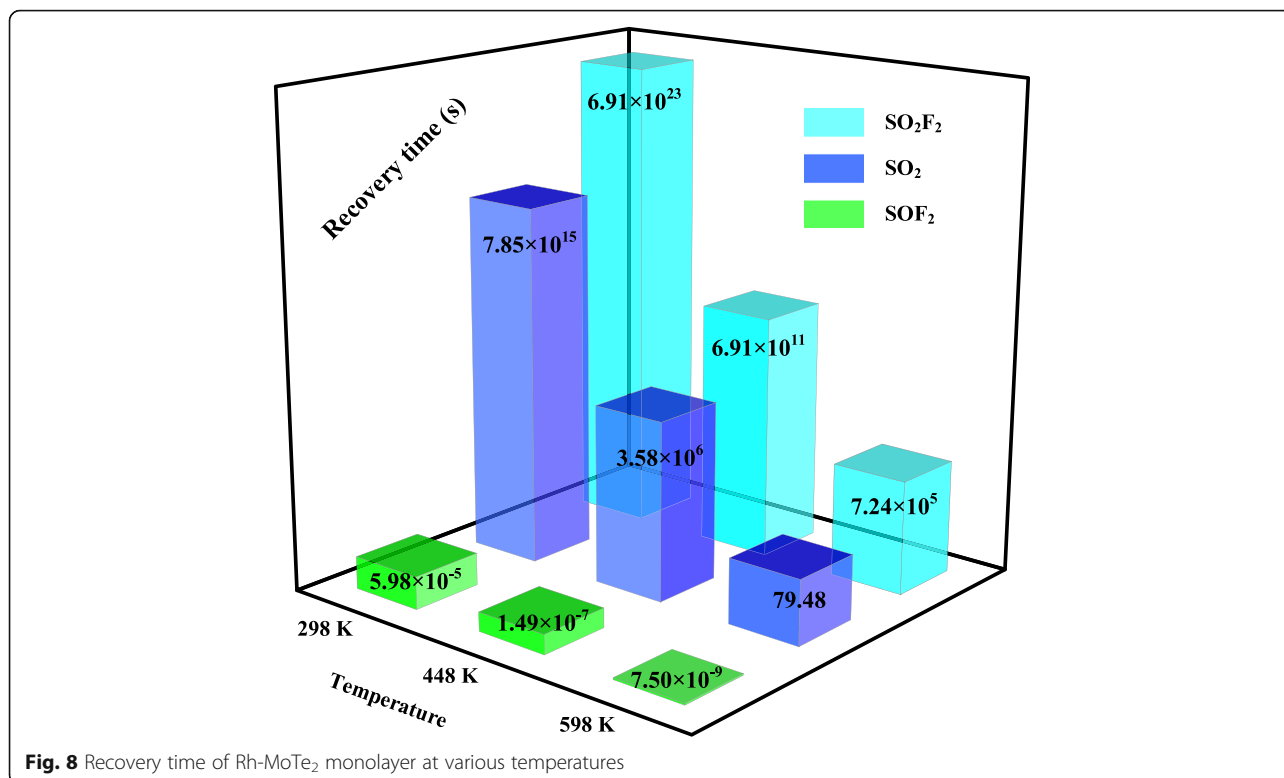


Fig. 8 Recovery time of Rh-MoTe₂ monolayer at various temperatures

SO_2F_2 , followed by the SO_2 and the last one comes to SOF_2 . This order is in accordance with those analysis of adsorption parameter and electronic behavior. Based on these results, it is hopeful that Rh-MoTe₂ monolayer could realize sensitive detection of SO_2 and SO_2F_2 at room temperature.

The recovery property is also important to evaluate the reusability of the gas sensor, and to reduce the recovery time (τ) of gas desorption from certain surfaces, heating technique is usually considered since the recovery time is related to the temperature (T), formulated as [45] $\tau = A^{-1}e^{(-E_a/K_B T)}$. In this formula, A is the attempt frequency referring to 10^{12} s^{-1} [46], E_a is the potential barrier, determined as equivalent as E_{ad} in this work, and K_B is the Boltzmann constant ($8.318 \times 10^{-3} \text{ kJ}/(\text{mol}\cdot\text{K})$).

Based on the formula, the recovery behavior of Rh-MoTe₂ monolayer at 298, 448, and 598 K is portrayed in Fig. 8. It can be seen from this figure that the desorption of SO_2F_2 and SO_2 at room temperature are extremely difficult, while for SOF_2 the recovery time is quite short due to its weak binding force with the Rh-doped surface. Through heating, the recovery time for SO_2F_2 or SO_2 desorption is pronouncedly reduced, and when the temperature increases to 598 K, the recovery time in SO_2 system (79.48 s) becomes favorable which allow its reusability in several minutes. This supports the potential of Rh-MoTe₂ monolayer as a reusable gas sensor for

detecting SO_2 . On the other hand, the long recovery time for SO_2F_2 desorption at 598 K (7.24×10^5) also reflects the strong chemisorption here. Although continuing to increase the temperature can further reduce the recovery time, the thermostability of the sensing material and the high energy consumption in sensing application would be another problem. Given all these, Rh-MoTe₂ monolayer is not suitable as a sensor for SOF_2 detection. However, it provides us another thought to propose Rh-MoTe₂ monolayer as a gas adsorbent to scavenge this noxious gas in SF_6 insulation devices, thus guaranteeing their safe operation. Moreover, this part of analysis from another aspect reveals the inappropriateness to explore Rh-MoTe₂ monolayer as a SO_2F_2 sensor given the weak interaction with the surface.

Optical Behavior of Rh-MoTe₂ Monolayer upon Gas Adsorption

Given the desirable optical property of MoTe₂ monolayer, the calculation of the dielectric function of Rh-MoTe₂ monolayer upon gas adsorption is conducted, as displayed in Fig. 9, to illustrate its possibility as an optical gas sensor.

From Fig. 9, it is seen that there have three main adsorption peaks for the isolated Rh-MoTe₂ monolayer, localizing at 148, 389, and 1242 nm, among which the former two distance are in the range of ultraviolet ray and the last one is in the range of infrared ray. After gas

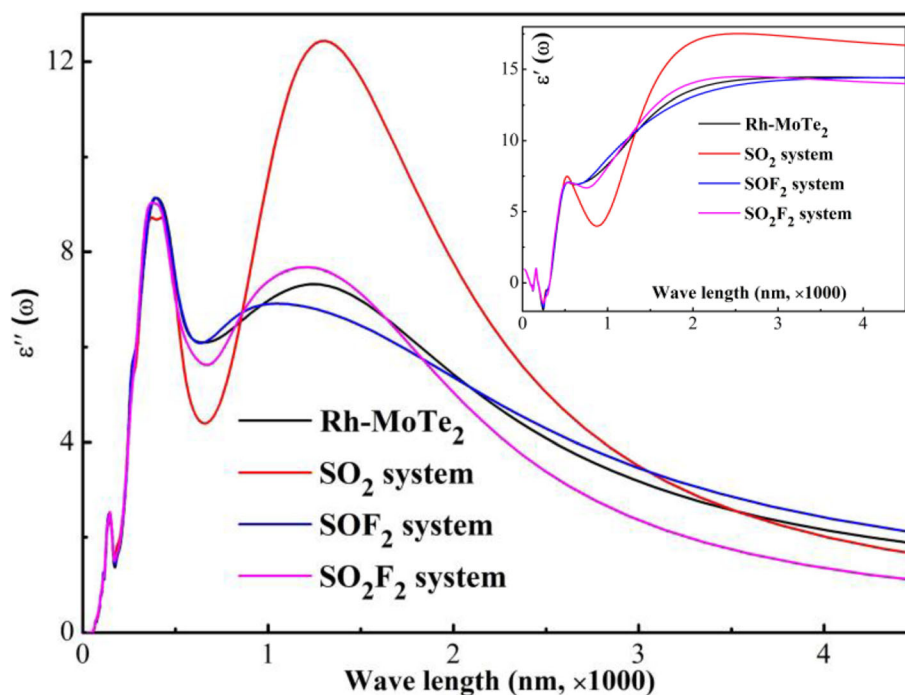


Fig. 9 Dielectric function of Rh-MoTe₂ monolayer

adsorption, the peaks in ultraviolet range suffer small deformation and that in infrared range undergoes significant deformation. Detailedly, the peak intensity at 1242 nm decreases after SOF_2 adsorption whereas increases after SO_2 and SO_2F_2 adsorption, and the blue shift could also be identified in the SOF_2 system. Therefore, it could be assumed that Rh-MoTe₂ monolayer is a promising optical sensor for sensitive and selective detection of three gases by infrared device.

In short, it is worth adding that this work makes a progressive research for proposing novel nanomaterials to realize the detection of SF_6 decomposed species through various techniques, which would be significant to fulfil the evaluation of SF_6 insulation devices in an easy and high-efficiency manner.

Conclusions

In this paper, the potential application of Rh-MoTe₂ monolayer as a gas sensor for detection of SF_6 decomposed species is explored, which mainly contains two aspects: (1) Rh doping behavior on the intrinsic MoTe₂ monolayer and (2) adsorption and sensing behaviors of Rh-MoTe₂ monolayer upon SO_2 , SOF_2 , and SO_2F_2 . It is found that the Rh dopant prefers to be doped on the MoTe₂ surface through the T_{Mo} site with E_b of -2.69 eV, exerting great electron hybridization with the Te atoms. The adsorption performance of Rh-MoTe₂ monolayer upon three gases are in order as $\text{SO}_2\text{F}_2 > \text{SO}_2 > \text{SOF}_2$, in which chemisorption is identified in SO_2F_2 and SO_2 systems while physisorption in SOF_2 system, as further supported by the DOS analysis. Rh-MoTe₂ monolayer is a promising resistance-type gas sensor for recycle detection of SO_2 with a response of 76.3%, is a desirable adsorbent for SO_2F_2 removal from the SF_6 insulation device, and is promising as an optical sensor for selective detection of three gases. All in all, Rh-MoTe₂ monolayer is a potential sensing material for detection of SF_6 decomposed species. This work is meaningful to propose novel nano-sensing material and to realize the effective evaluation of SF_6 insulation devices in an easy and high-efficiency manner.

Methods Section

This work means to explore novel 2D sensing materials using first-principle theory for application in electrical engineering, through detecting the SF_6 decomposed species to evaluate the operation status of high-voltage insulation devices.

Supplementary information

Supplementary information accompanies this paper at <https://doi.org/10.1186/s11671-020-03361-6>.

Additional file 1: Figure S1. Geometries of (a) SO_2 , (b) SOF_2 , and (c) SO_2F_2 . The black values are bond length while the orange values are bond angles.

Abbreviations

TMDs: Transition metal dichalcogenides; TM: Transition metal; CVD: Chemical vapor deposition; PBE: Perdew-Burke-Ernzerhof; GGA: Generalized gradient approximation; DNP: Double numerical plus polarization; Q_{Rh} : Atomic charge of Rh dopant; Q_i : Molecular charge of adsorbed molecules; E_b : Binding energy; MSC: Most stable configuration; EDD: Electron deformation density; BS: Band structure; DOS: Density of state; E_{ad} : Adsorption energy; D : Bond length; FMO: Frontier molecular orbitals; HOMO: Highest occupied molecular; LUMO: Lowest unoccupied molecular orbital

Acknowledgments

We acknowledge the financial support from the National Natural Science Foundation of China (no. 11572065), and Fundamental Research Funds for the Central Universities (grant no. SWU120001).

Authors' Contributions

Hongliang Zhu: writing; Hao Cui: editing and guidance; Dan He and Ziwen Cui: polishing; Xiang Wang: data analysis. Hao Cui and Hongliang Zhu contribute equally to this work. The author(s) read and approved the final manuscript.

Availability of Data and Materials

The data at present cannot be shared because they are still in study in our following research.

Consent for Publication

Not applicable

Competing Interests

The authors declare no conflict of interest.

Author details

¹Key Laboratory of Biorheological Science and Technology, Ministry of Education, College of Bioengineering, Chongqing University, Chongqing 400044, China. ²College of Artificial Intelligence, Southwest University, Chongqing 400715, China. ³State Key Laboratory of Power Transmission Equipment & System Security and New Technology, Chongqing University, Chongqing 400044, China. ⁴Chongqing New Oriental School, Chongqing 400030, China. ⁵College of Mobile Telecommunications, Chongqing University of Posts and Telecommunications, Chongqing 401520, China.

Received: 24 March 2020 Accepted: 28 May 2020

Published online: 15 June 2020

References

- Chen D, Zhang X, Tang J, Li Y, Cui Z, Zhou Q (2019) Using single-layer HfS₂ as prospective sensing device toward typical partial discharge gas in SF₆-based gas-insulated switchgear. *IEEE Transactions on Electron Devices* 66: 689–695
- Z. Xiaoxing, Y. Lei, W. Xiaoping, H. Weihua, Experimental sensing and density functional theory study of H₂S and SO₂ adsorption on Au-modified graphene, *Advanced Science*, (2015).
- Wang X, Zhi C, Li L, Zeng H, Li C, Mitome M, Golberg D, Bando Y (2011) "Chemical blowing" of thin-walled bubbles: high-throughput fabrication of large-area. Few-Layered BN and Cx-BN Nanosheets, *Advanced Materials* 23: 4072–4076
- Cui H, Chen D, Zhang Y, Zhang X (2019) Dissolved gas analysis in transformer oil using Pd catalyst decorated MoSe₂ monolayer: a first-principles theory. *Sustain Mater Technol* 20:e00094
- Cui H, Zhang X, Zhang G, Tang J (2019) Pd-doped MoS₂ monolayer: a promising candidate for DGA in transformer oil based on DFT method. *Appl Surf Sci* 470:1035–1042
- Cooke CM, Velazquez R (2006) The insulation of ultra-high-voltage in coaxial systems using compressed SF₆ gas. *IEEE Transactions on Power Apparatus & Systems* 96:1491–1497
- Zhang X, Zhang J, Jia Y, Xiao P, Tang J (2012) TiO₂ nanotube array sensor for detecting the SF₆ decomposition product SO₂. *Sensors* 12:3302–3313
- Zhang X, Dai Z, Wei L, Liang N, Wu X (2013) Theoretical calculation of the gas-sensing properties of Pt-decorated carbon nanotubes. *Sensors* 13: 15159–15171

9. Zhang X, Dai Z, Chen Q, Tang J (2014) A DFT study of SO₂ and H₂S gas adsorption on Au-doped single-walled carbon nanotubes. *Phys Scr* 89: 065803
10. Y. Gui, C. Tang, Q. Zhou, L. Xu, Z. Zhao, X. Zhang, The sensing mechanism of N-doped SWCNTs toward SF₆ decomposition products: A first-principle study, *Applied Surface Science*, 440 (2018).
11. D. Zhang, J. Wu, P. Li, Y. Cao, Room-temperature SO₂ gas-sensing properties based on a metal-doped MoS₂ nanoflower: an experimental and density functional theory investigation, *Journal of Materials Chemistry A*, 5 (2017).
12. Gui Y, Liu D, Li X, Tang C, Zhou Q (2019) DFT-based study on H₂S and SO₂ adsorption on Si-MoS₂ monolayer. *Results in Physics* 13:102225
13. Wei H, Gui Y, Kang J, Wang W, Tang C (2018) A DFT study on the adsorption of H₂S and SO₂ on Ni doped MoS₂ monolayer. *Nanomaterials* 8:646
14. Vedaiei SS, Nadimi E (2019) Gas sensing properties of CNT-BNNT-CNT nanostructures: a first principles study. *Appl Surf Sci* 470:933–942
15. Zhou J, Lin J, Huang X, Zhou Y, Chen Y, Xia J, Wang H, Xie Y, Yu H, Lei J (2018) A library of atomically thin metal chalcogenides. *Nature* 556:355–359
16. Zhou L, Xu K, Zubair A, Zhang X, Ouyang F, Palacios T, Dresselhaus MS, Li Y, Kong J (2017) Role of molecular sieves in the CVD synthesis of large-area 2D MoTe₂. *Adv Funct Mater* 27:1603491
17. Empante TA, Zhou Y, Klee V, Nguyen AE, Lu IH, Valentin MD, Naghibi Alvallar SA, Preciado E, Berges AJ, Merida CS (2017) Chemical vapor deposition growth of few-layer MoTe₂ in the 2H, 1T', and 1T phases: tunable properties of MoTe₂ films. *ACS Nano* 11:900–905
18. Z. Feng, Y. Xie, J. Chen, Y. Yu, S. Zheng, R. Zhang, Q. Li, X. Chen, C. Sun, H. Zhang, Highly sensitive MoTe₂ chemical sensor with fast recovery rate through gate biasing, *2d Materials*, 4 (2017) 025018.
19. Chen D, Zhang X, Tang J, Cui Z, Cui H (2019) Pristine and Cu decorated hexagonal InN monolayer, a promising candidate to detect and scavenge SF₆ decompositions based on first-principle study. *J Hazard Mater* 363:346–357
20. Shao P, Kuang X-Y, Ding L-P, Yang J, Zhong M-M (2013) Can CO₂ molecule adsorb effectively on Al-doped boron nitride single walled nanotube? *Appl Surf Sci* 285:350–356
21. Zhou X, Chu W, Zhou Y, Sun W, Xue Y (2018) DFT simulation on H₂ adsorption over Ni-decorated defective h-BN nanosheets. *Appl Surf Sci* 439: 246–253
22. Chopra NG, Luyken R, Cherrey K, Crespi VH, Cohen ML, Louie SG, Zettl A (1995) Boron nitride nanotubes. *Science* 269:966–967
23. Yuwen L, Xu F, Xue B, Luo Z, Zhang Q, Bao B, Su S, Weng L, Huang W, Wang L (2014) General synthesis of noble metal (Au, Ag, Pd, Pt) nanocrystal modified MoS₂ nanosheets and the enhanced catalytic activity of Pd-MoS₂ for methanol oxidation. *Nanoscale* 6:5762–5769
24. Giovanni M, Poh HL, Ambrosi A, Zhao G, Sofer Z, Šaněk F, Khezri B, Webster RD, Pumera M (2012) Noble metal (Pd, Ru, Rh, Pt, Au, Ag) doped graphene hybrids for electrocatalysis. *Nanoscale* 4:5002–5008
25. Sun YC, Kim Y, Chung HS, Kim AR, Kwon JD, Park J, Kim YL, Kwon SH, Hahn MG, Cho B (2017) Effect of Nb doping on chemical sensing performance of two-dimensional layered MoSe₂. *ACS Appl Mater Interfaces* 9:3817–3823
26. Cui H, Zhang G, Zhang X, Tang J (2019) Rh-doped MoSe₂ as toxic gas scavenger: a first-principles study. *Nanoscale Advances* 2019:772–780
27. Cui H, Zhang X, Yao Q, Miao Y, Tang J (2018) Rh-doped carbon nanotubes as a superior media for the adsorption of O₂ and O₃ molecules: a density functional theory study. *Carbon Letters* 28:55–59
28. Delley B (2000) From molecules to solids with the DMol3 approach. *J Chem Phys* 113:7756–7764
29. Tkatchenko A, DiStasio RA Jr, Head-Gordon M, Scheffler M (2009) Dispersion-corrected Møller-Plesset second-order perturbation theory. *J Chem Phys* 131:171–171
30. Perdew JP, Burke K, Ernzerhof M (1996) Generalized gradient approximation made simple. *Phys Rev Lett* 77:3865–3868
31. Delley B (2002) Hardness conserving semilocal pseudopotentials. *Phys Rev B Condens Matter* 66:155125
32. Cui H, Zhang X, Zhang J, Zhang Y (2019) Nanomaterials-based gas sensors of SF₆ decomposed species for evaluating the operation status of high-voltage insulation devices. *High Voltage* 4:242–258
33. Cui H, Jia P, Peng X (2020) Adsorption of SO₂ and NO₂ molecule on intrinsic and Pd-doped HfSe₂ monolayer: a first-principles study. *Appl Surf Sci* 513:145863
34. W. Ju, T. Li, X. Su, H. Li, X. Li, D. Ma, Au cluster adsorption on perfect and defective MoS₂ monolayers: structural and electronic properties, *Physical Chemistry Chemical Physics*, 19 (2017).
35. P. Wu, N. Yin, P. Li, W. Cheng, M. Huang, The adsorption and diffusion behavior of noble metal adatoms (Pd, Pt, Cu, Ag and Au) on a MoS₂ monolayer: a first-principles study, *Physical Chemistry Chemical Physics*, 19 (2017).
36. Cui H, Chen D, Yan C, Zhang Y, Zhang X (2019) Repairing the N-vacancy in an InN monolayer using NO molecules: a first-principles study. *Nanoscale Advances* 1:2003–2008
37. Pyykkö P, Atsumi M (2009) Molecular single-bond covalent radii for elements 1–118. *Chemistry* 15:186–197
38. Lezama IG, Arora A, Ubaldini A, Barreteau C, Giannini E, Potemski M, Morpurgo AF (2015) Indirect-to-direct band gap crossover in few-layer MoTe₂. *Nano Lett* 15:2336–2342
39. Cui H, Jia P, Peng X, et al. (2020) Adsorption and sensing of CO and C₂H₂ by S-defected SnS₂ monolayer for DGA in transformer oil: A DFT study. *Materials Chemistry and Physics* 249:123006
40. R.E. Ambrusi, C.R. Luna, M.G. Sandoval, P. Bechthold, M.E. Pronato, A. Juan, Rhodium clustering process on defective (8,0) SWCNT: analysis of chemical and physical properties using density functional theory, *Applied Surface Science*, 425 (2017).
41. Cui H, Liu T, Zhang Y, Zhang X (2019) Ru-InN Monolayer as a gas scavenger to guard the operation status of SF₆ insulation devices: a first-principles theory. *IEEE Sensors J* 19:5249–5255
42. Krekelberg WP, Greeley J, Mavrikakis M (2004) Atomic and molecular adsorption on Ir(111). *J Phys Chem B* 108:987–994
43. Verlag S (2006) Semiconductor physical electronics. *Semiconductor Physical Electronics* 28:363–364
44. Cui H, Yan C, Jia P, Cao W (2020) Adsorption and sensing behaviors of SF₆ decomposed species on Ni-doped C₃N monolayer: a first-principles study. *Appl Surf Sci* 512:145759
45. Zhang YH, Chen YB, Zhou KG, Liu CH, Zeng J, Zhang HL, Peng Y (2009) Improving gas sensing properties of graphene by introducing dopants and defects: a first-principles study. *Nanotechnology* 20:185504
46. Peng S, Cho K, Qi P, Dai H (2004) Ab initio study of CNT NO₂ gas sensor. *Chem Phys Lett* 387:271–276

Publisher's Note

Springer Nature remains neutral with regard to jurisdictional claims in published maps and institutional affiliations.

Submit your manuscript to a SpringerOpen® journal and benefit from:

- Convenient online submission
- Rigorous peer review
- Open access: articles freely available online
- High visibility within the field
- Retaining the copyright to your article

Submit your next manuscript at ► [springeropen.com](https://www.springeropen.com)